WENO semi-lagrangian particle methods

Georges-Henri Cottet

WENO semi-lagrangian particle methods

G.H. Cottet
Université Grenoble Alpes and CNRS, Laboratoire Jean-Kuntzmann

January 23, 2024

1 Why WENO particles

Semi-lagrangian (SL) particle methods are very efficient to solve transport equations, in particular in the context of vortex methods [1, 7]. When used with appropriate remeshing kernels they lead to high order, conservative, methods. They are stable under the sole condition that particle paths do not cross, a condition that can lead to significant savings compared to the CFL condition that grid-based methods need to satisfy (see [4] for an analysis and numerical illustrations).

However, like all high order methods, they can suffer oscillations, overshoots or undershoots due to the fact that they do not satisfy a maximum principe. In many situations this is not a problem. However in some cases it is important to guarantee, say, the positivity of the solution. In the recent work [3] the use of high order semi-lagrangian particle methods proved very efficient, both in terms of accuracy and computational time, to solve the Vlasov equation in up to 6 dimensions. For the examples in plasma physics studied in that paper, the fact that the density functions was not guaranteed to be positive affected only rare particles and did not impact in any way the quality of the solution. Furthermore clipping negative parts of the density function did not change the results. On the contrary, the example given in that reference, in the context of astrophysics, consisting of two density blobs with stiff profiles merging with each other was of a different nature, although based on the same set of equations. In that case, negative values of the density were found in a significant number of particles and could not be discarded. This is the consequence of the stiff profile of the density used in this example. At least in that case, it seems that a semi-lagrangian method which would minimize oscillations while keeping high order would certainly be beneficial.

2 Prior works

The issue just outlined was already considered in the paper [2, 6]. In these works, the authors build on the analogy between semi-lagrangian (SL in brief) particle methods and finite-difference methods to design TVD particle methods. More precisely, for CFL less that 1 SL particle methods using a remeshing kernel preserving the 3 (resp 2) first moment are equivalent to the Lax-Wendroff (resp

upwind) finite-difference scheme. TVD (for Total Variation Diminishing) finite-difference schemes are built by combining Lax-Wendroff and upwind schemes using limiters based on the variations of the solution. Using the analogy just mentioned, it is possible to translate the resulting TVD finite-difference schemes into TVD remeshing kernels for SL particle methods.

What is remarkable, is that the methods retain their TVD character even for time steps not constrained by CFL conditions. In [6] the possibility to use these methods with large time-steps allowed to perform in some cases even better than high order WENO finite-difference methods, although they were nominally only first order by definition. However, in other cases, when the CFL number was small, these methods proved to produce excessive numerical dissipation, more inline with what should be expected. This makes it desirable to extend the construction of TVD SL particle methods to WENO SL particle methods. Let us finally mention a more recent paper [8]) where the authors construct WENO schemes for forward semi-lagrangian methods and apply these to 1D Vlasov-Poisson equations and transport equations with constant velocity.

3 WENO semi-lagrangian particle methods

We will consider in the sequel the following 1D transport equation

$$u_t + (au)_x = 0, \tag{1}$$

with periodic boundary condition in $[0, 1]$, where a is a smooth velocity field.

Let us first recall how finite-difference WENO schemes work, and consider the case where a is a non negative constant. We start with the the semi-discrete transport equation

$$\frac{u^{n+1} - u^n}{\Delta t} + a^n u_x^n = 0. \tag{2}$$

At node i of a discretization of the domain, the equation is therefore

$$\frac{u_i^{n+1} - u_i^n}{\Delta t} + a_i^n (u_x)_i^n = 0. \tag{3}$$

A fifth-order WENO scheme uses the values

$$\{u_{i-3}, u_{i-2}, u_{i-1}, u_i, u_{i+1}, u_{i+2}\}$$

to determine an approximation of u_x at the node x_i. In the case when $a < 0$ this stencil would be shifted to the right to ensure the proper upwinding for stability.

Following [9], we set

$$v_1 = \frac{u_{i-2} - u_{i-3}}{\Delta x}, \ ; v_2 = \frac{u_{i-1} - u_{i-2}}{\Delta x}, \ ; v_3 = \frac{u_i - u_{i-1}}{\Delta x}, v_4 = \frac{u_{i+1} - u_i}{\Delta x}, \ ; v_5 = \frac{u_{i+2} - u_{i+1}}{\Delta x}.$$

Then

$$\partial_x u^1 = \frac{v_1}{3} - \frac{7v_2}{6} + \frac{11v_3}{6}, \tag{4}$$

$$\partial_x u^2 = -\frac{v_2}{6} + \frac{5v_3}{6} + \frac{v_4}{3}, \tag{5}$$

$$\partial_x u^3 = \frac{v_3}{3} + \frac{5v_4}{6} - \frac{v_5}{6}, \tag{6}$$

are third-order approximations of u_x. It was noticed that by taking an optimal convex combination of the three quantities above to approximate u_x, one could reach fifth order in regions where u is smooth.

We therefore take an approximation of the form

$$(\partial_x u^-)_i \approx \omega_1 \partial_x u^1 + \omega_2 \partial_x u^2 + \omega_3 \partial_x u^3,$$

where $0 \leq \omega_k \leq 1$ are some weights taking into account the regularity of the solution on the corresponding stencils and satisfying $\omega_1 + \omega_2 + \omega_3 = 1$. In regions where u is smooth, it can be easily checked that the optimal choice is $\omega_1 = 0.1$, $\omega_2 = 0.6$ et $\omega_3 = 0.3$. WENO schemes are based on the determination of the weights ω_k on the basis of some smoothness indicators of the numerical solution. More precisely, [9] first writes

$$S_1 = \frac{13}{12}(v_1 - 2v_2 + v_3)^2 + \frac{1}{4}(v_1 - 4v_2 + 3v_3)^2, \tag{7}$$

$$S_2 = \frac{13}{12}(v_2 - 2v_3 + v_4)^2 + \frac{1}{4}(v_2 - v_4)^2, \tag{8}$$

$$S_3 = \frac{13}{12}(v_3 - 2v_4 + v_5)^2 + \frac{1}{4}(3v_3 - 4v_4 + v_5)^2, \tag{9}$$

and then defines

$$\alpha_1 = \frac{0.1}{(S_1 + \varepsilon)^2}, \quad \alpha_2 = \frac{0.6}{(S_2 + \varepsilon)^2}, \quad \alpha_3 = \frac{0.3}{(S_3 + \varepsilon)^2}, \tag{10}$$

where $\varepsilon > 0$ is a (very) small parameter, and finally consider the weights

$$\omega_k = \frac{\alpha_k}{\alpha_1 + \alpha_2 + \alpha_3}, \quad k = 1, 2, 3.$$

A similar approach can be followed to construct WENO SL particle methods. Generally speaking a SL particle method using the remeshing kernel Λ can be written as follows

$$u_i^{n+1} = S_i(u^n) \equiv \sum_j u_j^n \Lambda\left(\frac{x_j^{n+1} - x_i}{\Delta x}\right) \tag{11}$$

where $x_i = i\Delta x$ and x_j^{n+1} denotes the location at time t_{n+1} of the particle which was located at time t_n at x_j. This location depends for non constant velocity on the time-stepping scheme. Λ denotes an interpolating kernel which must satisfy moment and regularity properties.

We will consider here the case of the so-called M_4' remeshing scheme (or $\Lambda_{2,1}$ according to the terminology in [4]). This kernel conserves the 3 first moments of the particle distribution and in of class C^1. It is therefore second order wherever the density of particles does not vary from one cell to the next, and first order elsewhere [4]. This kernel is given by the formulas

$$\Lambda_{2,1}(x) = \begin{cases} 1 - \frac{5}{2}|x|^2 + \frac{3}{2}|x|^3 & 0 \leqslant |x| < 1 \\ 2 - 4|x| + \frac{5}{2}|x|^2 - \frac{1}{2}|x|^3 & 1 \leqslant |x| < 2 \\ 0 & 2 \leqslant |x| \end{cases} \tag{12}$$

The particle method using this kernel assigns weights to the 4 neighboring points (see Table 1) with the following coefficient values :

$$\alpha = \frac{1}{2}\lambda(1-\lambda)^2 \;;,\; ;\beta = 1 - \frac{5}{2}\lambda^2 + \frac{3}{2}\lambda^3 \;;,\; ;\gamma = \lambda(\frac{1}{2} + 2\lambda - \frac{3}{2}\lambda^2) \;;,\; ;\delta = \frac{1}{2}(\lambda-1)\lambda^2,$$

where $\lambda = a\Delta t/\Delta x$. If a is constant and $0 \leq a\Delta t \leq \Delta x$, this method is equivalent to the following finite-difference scheme

$$u_i^{n+1} = \alpha_{i+1} + \beta_i + \gamma_{i-1} + \delta_{i-2} \tag{13}$$

that is

$$\begin{aligned} u_i^{n+1} &= u_{i-2}^n \left[\frac{1}{2}(\lambda-1)\lambda^2\right] + u_{i-1}^n \left[\lambda(\frac{1}{2} + 2\lambda - \frac{3}{2}\lambda^2\right] + u_i^n \left[1 - \frac{5}{2}\lambda^2 + \frac{3}{2}\lambda^3\right] - u_{i+1}^n \left[\frac{1}{2}\lambda(1-\lambda)^2\right] \\ &= u_i^n - \frac{\lambda}{2}(1-\lambda)^2(u_{i+1}^n - u_i^n) + \frac{\lambda}{2}(-1-3\lambda+2\lambda^2)(u_i^n - u_{i-1}^n) - \lambda^2(\lambda-1)(u_{i-1}^n - u_{i-2}^n) \\ &= u_i^n - \frac{\lambda}{2}(1-\lambda)^2 v_4 + \frac{\lambda}{2}(-1-3\lambda+2\lambda^2)v_3 - \lambda^2(\lambda-1)v_2, \end{aligned}$$

where v_2, v_3, v_4 have been defined above.

The above equation is similar to the time discrete approximation of the transport equation using the approximation (6) of u_x. It should be noted that this remeshing scheme implicitly involves some upwinding. In other words, if the velocity is negative, il will automatically adapt the equivalent finite-difference stencils to provide the correct upwinding.

To continue the derivation of WENO particle methods we now need remeshing schemes involving approximations similar to (4) and (6). This will be provided by left-sided and right-sided M_4' remeshing formulas. These formulas are given by the following kernels [5] :

$$\Lambda_{2,1}^l(x) = \begin{cases} 0 & x < -3 \\ -2 - 4(x+1) - \frac{5}{2}(x+1)^2 - \frac{1}{2}(x+1)^3 & -3 \leqslant x < -2 \\ 2(x+1) + \frac{7}{2}(x+1)^2 + \frac{3}{2}(x+1)^3 & -2 \leqslant x < -1 \\ 2(x+1) + \frac{1}{2}(x+1)^2 - \frac{3}{2}(x+1)^3 & -1 \leqslant x < 0 \\ 2 - \frac{3}{2}(x+1)^2 + \frac{1}{2}(x+1)^3 & 0 \leqslant x < 1 \\ 0 & 1 < x \end{cases} \tag{14}$$

$$\Lambda_{2,1}^r(x) = \begin{cases} 0 & x < -1 \\ -2 - \frac{3}{2}(x-1)^2 - \frac{1}{2}(x-1)^3 & -1 \leqslant x < 0 \\ -2(x-1) + \frac{1}{2}(x-1)^2 + \frac{3}{2}(x-1)^3 & -0 \leqslant x < 1 \\ -2(x-1) + \frac{7}{2}(x-1)^2 - \frac{3}{2}(x-1)^3 & 1 \leqslant x < 2 \\ -2 + 4(x-1) - \frac{5}{2}(x-1)^2 + \frac{1}{2}(x-1)^3 & 2 \leqslant x < 3 \\ 0 & 3 \leq x \end{cases} \tag{15}$$

Theses kernels in turn give formulas to compute the weights assigned to the neighboring points. Table 1 shows the weights assigned on particles with indices $i^\star - 2$ to $i^\star + 3$ from a particle originating

	$i^\star-2$	$i^\star-1$	$i^\star$	$i^\star+1$	$i^\star+2$	$i^\star+3$
$\Lambda^l_{2,1}$	α'_i	β'_i	γ'_i	δ'_i	0	0
$\Lambda_{2,1}$	0	α_i	β_i	γ_i	δ_i	0
$\Lambda^r_{2,1}$	0	0	α''_i	β''_i	γ''_i	δ''_i

	$i-3$	$i-2$	$i-1$	i	$i+1$	$i+2$
$\Lambda^l_{2,1}$			•	•	•	•
$\Lambda_{2,1}$		•	•	•	•	
$\Lambda^r_{2,1}$	•	•	•	•		

Table 1: Weights associated to the centered and one-sided $\Lambda_{2,1}$ kernels (left) and corresponding finite-difference stencils (right). See text for explanations.

at the node of index i, where $i^\star$ in the index of the grid point nearest to this particle on the left after advection.The coefficients $\alpha, \beta, \cdots$ (resp $\alpha', \beta', \cdots$, α", β", $\cdots$ are computed with the formula (12) (resp the formulas (14), (15)). The right part of the table shows the stencil of the equivalent finite-difference scheme at the grid-point i when $\lambda = a\Delta t/\Delta x \in [0, 1]$. If $\lambda < 0$ this stencil is inverted to account for the implicit upwinding in the remeshing scheme, so that all for stencils keep at least one upwind point.

To construct a WENO scheme we now need to combine these three remeshing schemes with coefficients depending on the regularity of the solution on the corresponding stencils. We first need to find an optimal combination of the remeshing kernels which, for smooth solutions, provides the best accuracy possible. For that we observe that for symmetry reasons the coefficients of the left and right kernels should be equal and the sum on the 3 coefficients should be one, which leaves only one coefficient to choose. We performed a numerical exploration of the parameter space and obtained that a linear combination of the kernels $\Lambda_{2,1}$, $\Lambda^l_{2,1}$ and $\Lambda^r_{2,1}$ with coefficients $c_m = 0.662$, $c_l = 0.169$ and $c_r = 0.169$, respectively, significantly improves the accuracy of the $\Lambda_{2,1}$ kernel (see Figure 1).

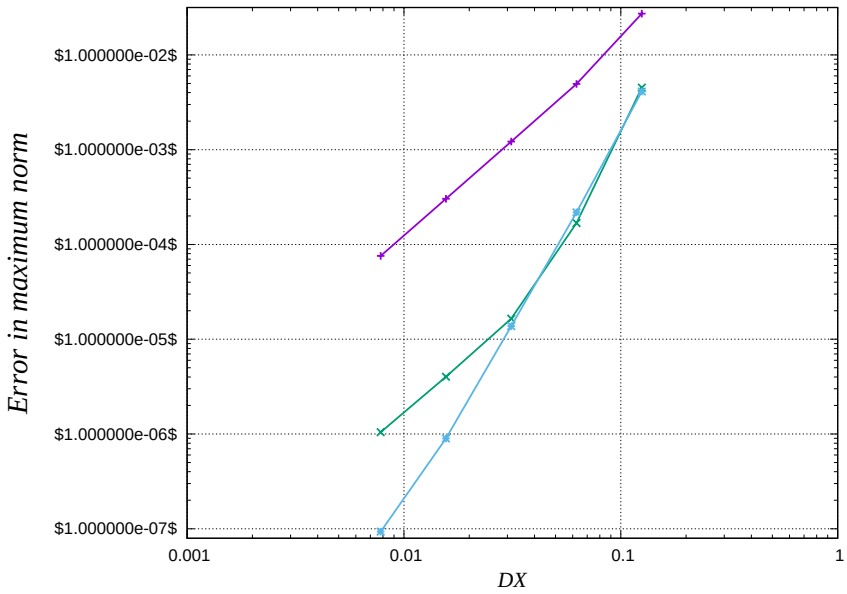

Figure 1: Error plot for $\Lambda_{2,1}$ (magenta curve), the combination $0.169\,\Lambda^l_{2,1} + 0.662\,\Lambda_{2,1} + 0.169\Lambda^r_{2,1}$ (green) and $\Lambda_{4,2}$ (blue)

To ponder these coefficients with smoothness indicators we next use the same formulas as in (7)-(9) and we make two remarks. We first observe that remeshing the particle originating at x_i with the kernel $\Lambda_{2,1}$ translates into a finite-difference scheme using the stencil $i-2, i-1, i, i+1$ (remember that we are in the case where $a > 0$). It should therefore be associated to smoothness indicator on this stencil. We next observe that the finite-difference scheme (13) associated with this kernel at the grid point x_i involves weights corresponding to particle i (weight β_i), $i+1$ (weight α_{i+1}), $i-1$ (weight γ_{i-1}) and $i-2$ (weight δ_{i-2}). Similarly the kernel $\Lambda^l_{2,1}$ should be associated with smoothness indicators on the stencil $i-1, i, i+1, i+2$ which should affect the weights α'_{i+2}, β'_{i+1}, γ'_i and δ'_{i-1}. And the kernel $\Lambda^r_{2,1}$ should be associated with smoothness indicators on the stencil $i-3, i-2, i, i+1$ which should affect the weights α''_i, β''_{i-1}, γ''_{i-2} and δ''_{i-3}.

Translating these remarks back to the remeshing scheme allows to determine the WENO formula to remesh the particle originating at x_i. It consists of adding at the corresponding grid points indicated in Table 1

- the weights $\alpha_i\, c_m\, \omega_2(i-1)$, $\beta_i\, c_m\, \omega_2(i)$, $\gamma_i\, c_m\, \omega_2(i+1)$, $\delta_i\, c_m\, \omega_2(i+2)$, where $\alpha, \beta, \gamma, \delta$ are associated to the kernel $\Lambda_{2,1}$
- the weights $\alpha'_i\, c_l\, \omega_3(i-2)$, $\beta'_i\, c_l\, \omega_3(i-1)$, $\gamma'_i\, c_l\, \omega_3(i)$, $\delta'_i\, c_l\, \omega_3(i+1)$, where $\alpha', \beta', \gamma', \delta'$ are associated to the kernel $\Lambda^l_{2,1}$
- the weights $\alpha''_i\, c_r\, \omega_1(i)$, $\beta''_i\, c_r\, \omega_1(i+1)$, $\gamma''_i\, c_r\, \omega_1(i+2)$, $\delta''_i\, c_r\, \omega_1(i+3)$, where $\alpha'', \beta'', \gamma'', \delta''$ are associated to the kernel $\Lambda^r_{2,1}$.

where the coefficients $\alpha, \beta, \gamma, \delta, \alpha', \beta', \gamma', \delta', \alpha'', \beta'', \gamma'', \delta''$ are depicted for each particle on Table 1. Note that the resulting method is not conservative as the smoothness coefficients can vary form one particle to the next. Note also that, although we have so far assumed a positive velocity, for the case of a negative velocity at particle i the implicit upwinding in the particle method ensures that it is not necessary to reverse the side of the stencils used to evaluate the smoothness coefficients.

4 Numerical illustrations

Let us first check our claim that, for smooth solutions the coefficients c_m, c_l and c_r provide improved accuracy for the kernel $c_m\Lambda_{2,1} + c_l\Lambda^l_{2,1} + c_r\Lambda^r_{2,1}$ over the original $\Lambda_{2,1}$ kernel. For that we consider the transport of a smooth sine wave with constant velocity. The velocity field is taken equal to 1 in the periodic box $[-1, +1]$. The error curves corresponding to $\Lambda_{2,1}$, $c_m\Lambda_{2,1} + c_l\Lambda^l_{2,1} + c_r\Lambda^r_{2,1}$ and the 4th order kernel $\Lambda_{4,2}$ are reported in Figure 1. The improved accuracy of $c_m\Lambda_{2,1} + c_l\Lambda^l_{2,1} + c_r\Lambda^r_{2,1}$ is clear (this combination is actually closer to the 4th order of $\Lambda_{4,2}$).

4.1 Linear advection

Figure 2 next compares the WENO scheme just defined with the original $\Lambda_{2,1}$ remeshing for a step function transported over a time $T = 2$ with a constant velocity. The improvement is clear.

The large overshoot and undershoot have be removed. In the comparison with the 4th order $\Lambda_{4,2}$ scheme, on can see that the oscillations following the overshoot have also been removed. In these experiments, the WENO particle scheme have been implemented with values of the smoothness indicators S_i obtained by formulas (7), (8), (9) with the coefficient 1/4 replaced by 0 (using the original coefficients only smears a little bit the fronts) and $\epsilon = 10^{-6}$. In this experiment the CFL number was equal to 0.6 but increasing this CFL number only improves results for both the original and the WENO particle method (remember that we are in the case of a constant velocity field, so that for particle methods, the larger the CFL number, the better the solution), with always a significant improvement of the WENO method.

We now consider a more challenging case when the velocity field is non constant. We choose

$$a(x) = 1 + \frac{1}{2}\sin(\pi x) \tag{16}$$

in the interval $[-1, +1]$. This velocity induces transport together with compression and dilatation, in a time-periodic fashion with period $T = 4\sqrt{3}$. The Figure 3 corresponds to the the transport of a double Heaviside function over a time T, compared to the exact solution (equal to the initial condition) and to the result provided by a finite-difference 5th-order WENO scheme. Both methods use $\Delta x = 0.01$, a RK3 time-stepping and a CFL number equal to 2, which is the maximum CFL allowed for stability in the finite-difference scheme. We also show the solutions at time $t = 3$ showing the compression and dilatation produced by the flow.

One can see the improvement of the particle method over the 5th order finite-difference method, which is actually surprising given that the particle method is based on a scheme which is only first order for a non-constant velocity field and that for CFL smaller than 1 the particle method reduces to a finite-difference method.

However when the CFL number increases one can see on Figure4 that oscillations appear near the maximum values of the solution. In this example the CFL number for the WENO particle method was 12.

To better control these oscillations for larger CFL, we found advisable to change the parameter ϵ in the equations 10. In the previous experiment, it was set to 10^{-6} and we now set it to the grid-size Δx.

Figure 5 and Figure 6 show comparaisons with the exact solution after time $t = 3T$, of the WENO semi-lagrangian particle methods, the 5th order finite-difference method and the original particle methods with the kernel $\Lambda_{4,2}$, for CFL values, for the particle methods, equal to 12 and 20 (the CFL value for the finite-difference method remains equal to its maximum value 2).

Two kind of observations ca be made from these experiments. The comparison with original seml-lagrangian particle methods shows that the WENO schemes at low or intermediate CFL numbers are able to get rid of most of the oscillations without creating notable excess numerical diffusion. At higher CFL number, some numerical diffusion appears. On the other hand, the semi-lagrangian WENO scheme compares well with the 5th order finite-difference WENO schemes, in particular at intermediate CFL numbers, with, at least in the test case used in the present study, less numerical diffusion and a better control of the overshoot.

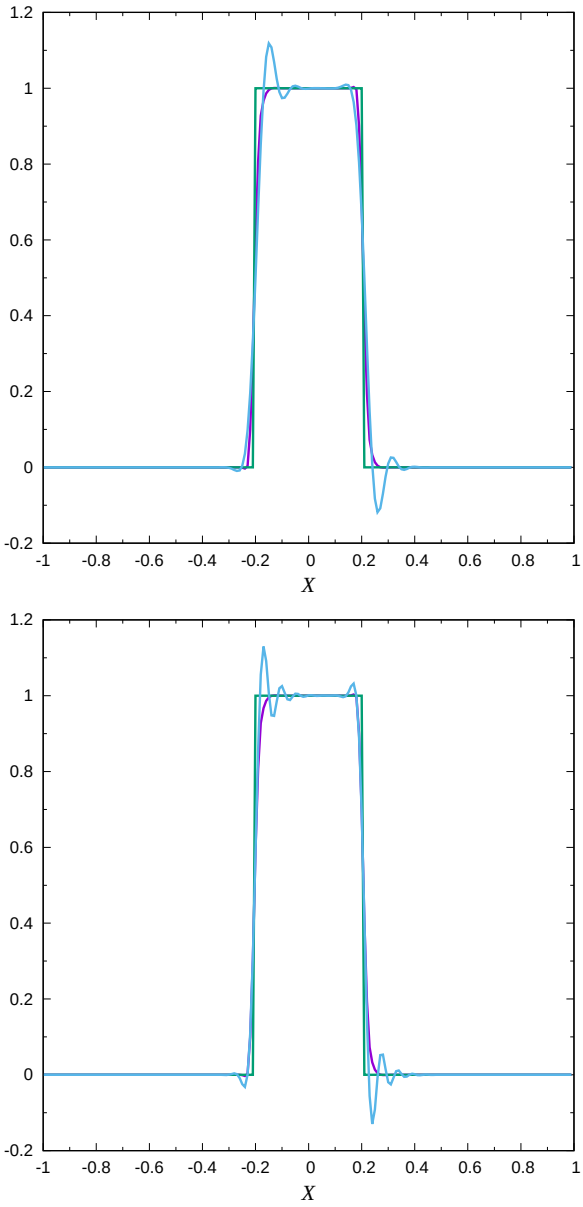

Figure 2: Comparison of particle WENO scheme (magenta curve) with exact solution (green curve) and classical particle methods with remeshing (blue curve), for the advection of a step function with constant velocity after one period. Top figure : blue curve is second order original $\Lambda_{2,1}$ remeshing kernel ; bottom figure : blue curve is 4th order $\Lambda_{4,2}$ remeshing .

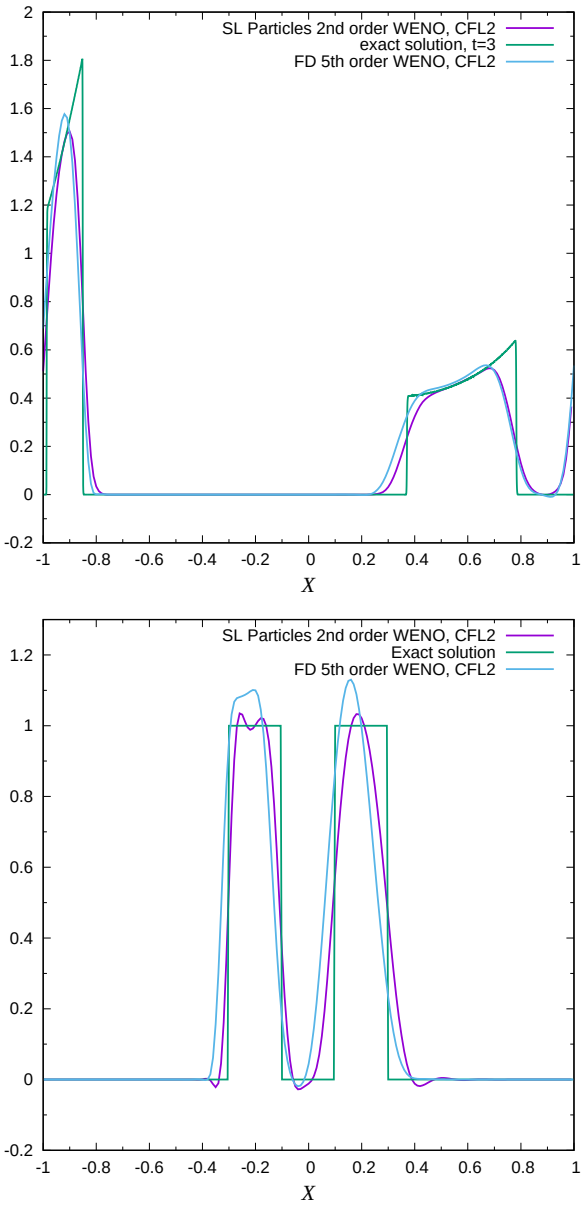

Figure 3: Comparison of tbe WENO particle method with exact solution (green) and finite-difference 5th order WENO at CFL 2 with $N = 200$ points for the advection of a double heaviside with the velocity field (16). Top picture : $t = 3$; bottom picture : $t = 3T = 4\sqrt{3}$

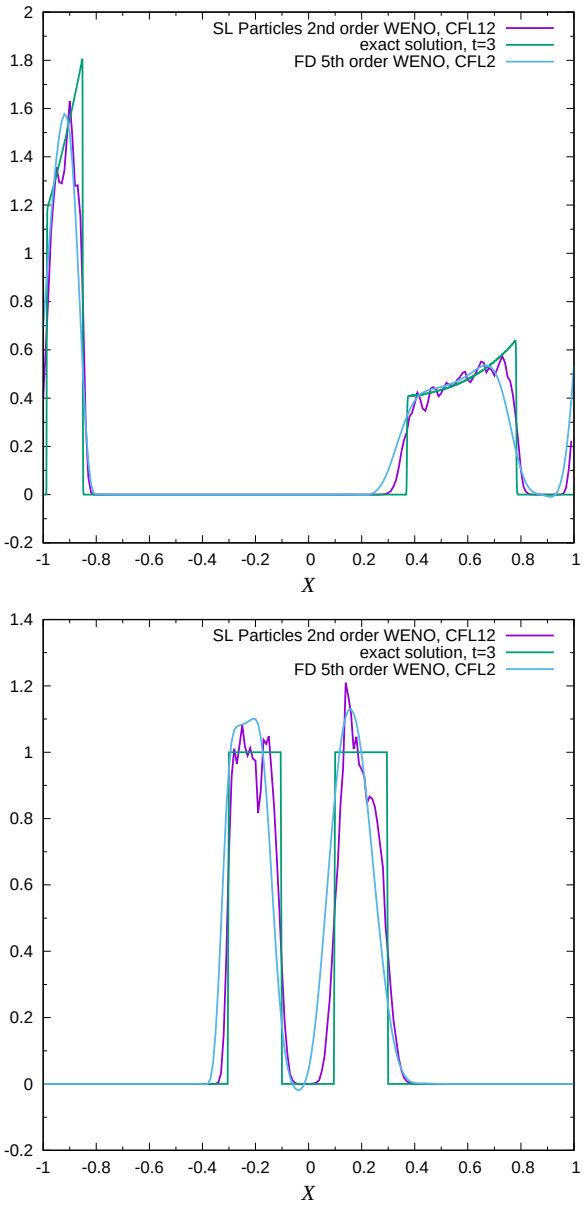

Figure 4: Comparison of the WENO particle method at CFL 12 with exact solution and finite-difference 5th order WENO (blue) at CFL 2 with $N = 200$ points for the advection of a double heaviside with the velocity field (16). Top picture : $t = 3$; bottom picture : $t = 3T = 4\sqrt{3}$

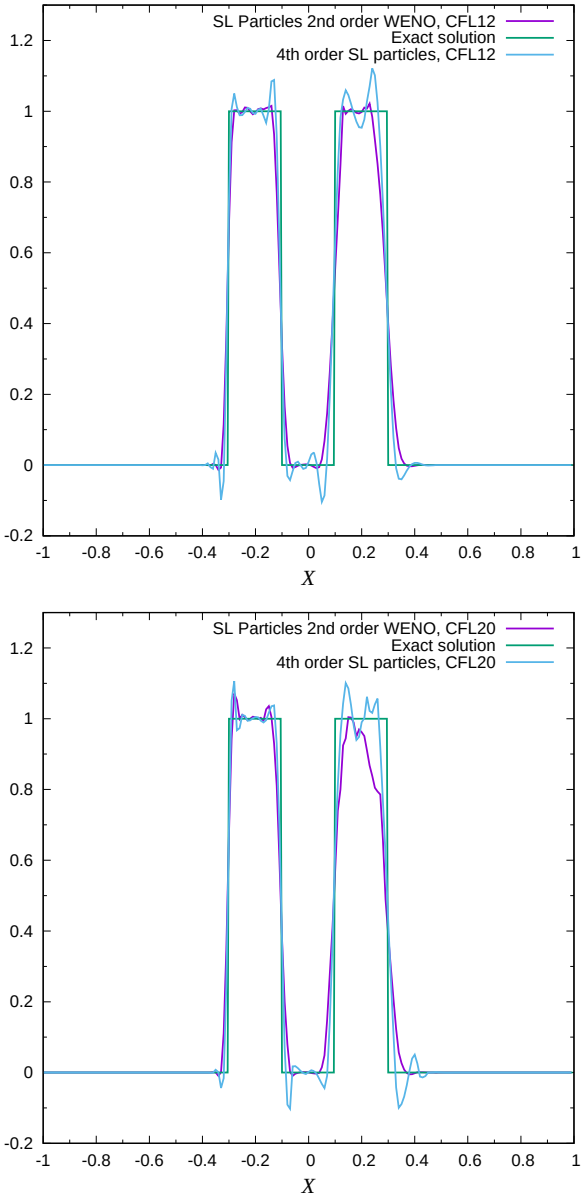

Figure 5: Comparison at $t = 3T$ of WENO particle method with the original semi-lagrangian particle method with kernel $\Lambda_{4,2}$, and exact solution for the advection of a double heaviside with velocity field of (16), when $\epsilon = \Delta x$ in (10). Top picture : CFL=12 ; bottom picture : CFL=20

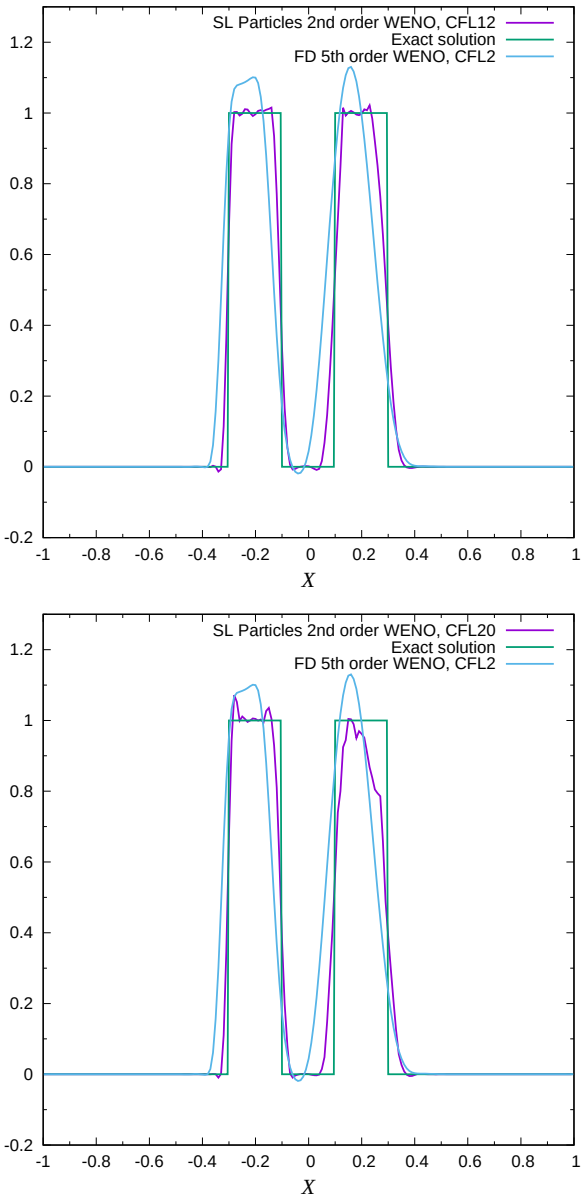

Figure 6: Comparison at $t = 3T$ of WENO particle method with 5th order WENO finite-difference scheme and exact solution, for the advection of a double heaviseide with velocity field of (16) for different values of the CFL number for the particle method, when $\epsilon = \Delta x$ in (10). Top picture : CFL=12 ; bottom picture : CFL=20

4.2 Burgers equation

We now consider the non-linear Burgers equation

$$u_t + (\frac{1}{2}u^2)x = 0, \text{ for } t > 0 \tag{17}$$

with periodic boundary conditions in $[0, 1]$. Following [2], to achieve second order in time, particles are advected at each time-step with velocity evaluated by the formula

$$v_j = \frac{1}{2}u_j \left(1 - \frac{1}{2}\Delta t(u_{j+1} - u_{j-1})\right)$$

In the above formula u_j and v_j respectively denote the solution and velocity value sat the particle with index j and Δt is the time-step. After advection, particles are remeshed with the formulas described in the previous section.

We consider the initial condition given by

$$u_0(x) = \begin{cases} 1 + \sin(6\pi(x - 1/3))/2 & \text{if } 1/3 \leq x \leq 2/3 \\ 1 & \text{otherwise.} \end{cases} \tag{18}$$

We compare the WENO particle method just defined with the exact solution and the TVD particle method developed in [2]. Figure 7 shows the time evolution of the total variation of the solution and Figure 8 gives the profile of the solution at time $t = 0.2$. In the TVD and WENO solution the number of particles is queal to 200 and the CFL number is 0.2. One can observe that the WENO

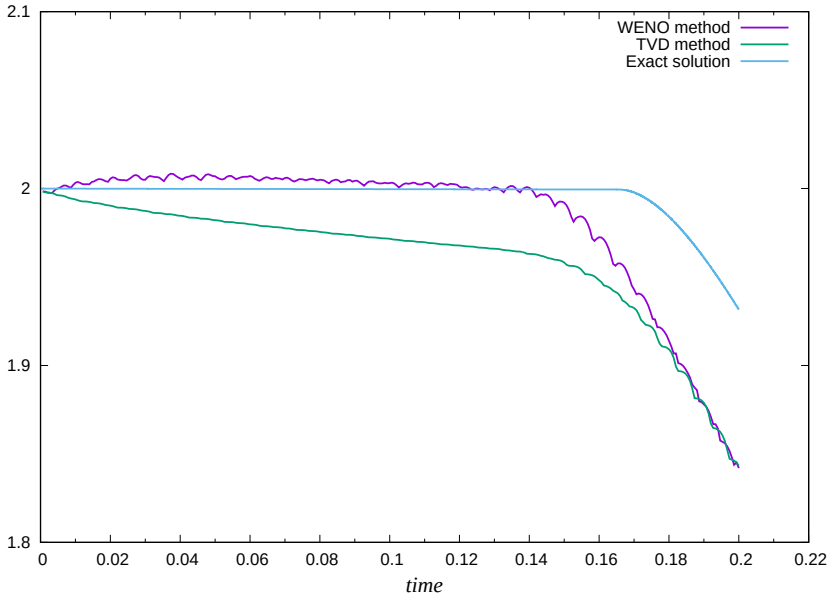

Figure 7: Comparison of WENO and TVD particle methods for the burgers equation at time $t = 0.2$ with initial condition (18). Time evolution of total variation

solution sticks better to the exact solution as long as the solution is smooth but when the shock

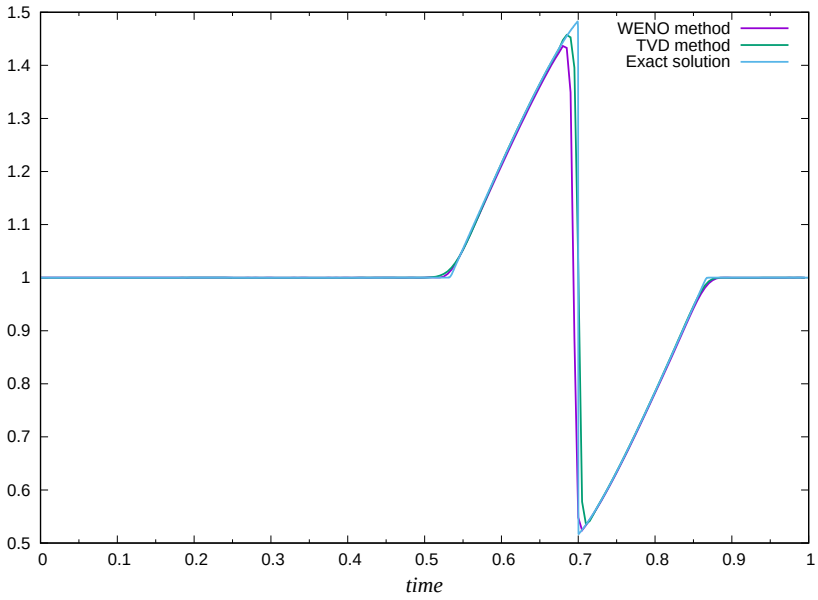

Figure 8: Comparison of WENO and TVD particle methods for the burgers equation at time $t = 0.2$ with initial condition(18). Solution profile at $t = 0.2$.

appears it produces results which are very similar to the TVD method. Shock tube experiments for 1d gas dynamics (not shown) lead to the same observation. Given that the WENO scheme is based on a remeshing formula that is essentially second order, this is not surprising.

5 Conclusions and outlook

We have designed a WENO extension of semi-lagrangian particle methods, based on the methodology developed in finite-difference methods. Despite the fact that are based on low order remeshing kernels the results obtained on a 1D test case with non constant velocity show that they outperform 5th order WENO finite-difference schemes over a significant range of CFL values. These results are encouraging and several extensions and applications can be considered.

The WENO schemes just derived are not conservative. In all our experiments, despite the large strain involved by deviation of the mass remained of the order of 1%. However, given that the original particle methods are conservative by nature it might be desirable to derive WENO schemes which preserve this feature.

Another direction of research would be to derive WENO formulas from higher order kernels and/or optimize coefficients for the smoothness indicators, which in the present study were directly borrowed from finite-difference formulas.

Concerning possible applications, a first class of applications would be to use WENO schemes to control unphysical maxima/minima in particle simulations. In particular, multiphase flows or

the stiff astrophysics case of the 6D Vlasov-Poisson equations already mentioned would be good candidates to test the method. Another class of applications concerns the use of WENO schemes to provide implicit Large Eddy Simulation models. This direction of research is rather classical in the finite-difference world, and it could lead to novel algorithms for accurate LES which would not be constrained by CFL conditions.

References

[1] P. Koumoutsakos and A. Leonard, *High-resolution simulations of the flow around an impulsively started cylinder using vortex methods*, J. Fluid Mech., **296**, 1–38, 1995.

[2] G.-H.Cottet and A. Magni, *TVD remeshing formulas for particle methods*, C. R. Math., **347** (23-24), 1367–1372, 2009.

[3] G.-H. Cottet Semi-Lagrangian particle methods for high-dimensional Vlasov-Poisson systems, Journal of Computational Physics, 365, 362-375, 2018.

[4] G.-H. Cottet, J.-M. Etancelin, F. Perignon and C. Picard, High order Semi-Lagrangian particles for transport equations : numerical analysis and implementation issues, ESAIM : Mathematical Modelling and Numerical Analysis, 48, 1029-1060, 2014.

[5] J.-B. Keck, personal communication

[6] A. Magni and G.-H. Cottet, Accurate, non-oscillatory remeshing schemes for particle methods, J. Comput. Phys., 231 (1), 152–172, 2012.

[7] P. Koumoutsakos, Inviscid Axisymmetrization of an Elliptical Vortex, Journal of Computational Physics, Volume 138, Issue 2, 1997, Pages 821-857

[8] David Sirajuddin, William N.G. Hitchon, A truly forward semi-Lagrangian WENO scheme for the Vlasov-Poisson system, Journal of Computational Physics, Volume 392, 2019, 619-665.

[9] C.W Shu, High order ENO and WENO schemes for computational fluid dynamics, in High-order methods for computational physics, 1999, 429–582, Springer.